06

The mechanical properties of metal-matrix composites Al−Mg processed by high-pressure torsion

© G.F. Korznikova,[1] R.Kh. Khisamov,[1] K.S. Nazarov,[1] G.R. Khalikova,[1] R.U. Shayakhmetov,[1] R.R. Kabirov,[1] R.R. Timiryaev ,[1] E.A. Korznikova,[1,2] T.I. Nazarova,[1] R.R. Mulyukov[1]

[1] Institute for Metal Superplasticity Problems Russian Academy of Sciences
450001 Ufa, Bashkortostan, Russia
[2] Ufa University of Science and Technology,
450076 Ufa, Russia
e-mail: gfkorznikova@gmail.com

Received July 14, 2023
Revised June 5, 2024
Accepted June 21, 2024

The results of studies of the evolution of the structure and tensile properties of Al−Mg system composites obtained by torsion at an increased pressure of up to 8 GPa and varying the number of rotations from 10 to 100 are presented. It is shown that the maximum number of rotations during deformation ensured a uniform structure and strength at the level of high-strength aluminum alloys.

Keywords: ultrafine-grained materials, tensile strength, microhardness, solid solution, low-temperature heat treatment.

DOI: 10.61011/TP.2024.08.59013.180-23

Introduction

Light alloys based on aluminum and magnesium are widely used as structural materials in the aerospace, automotive and electronics industries [1,2]. The demand for these materials is constantly growing, and the improvement of the properties of alloys based on the system of Al−Mg (magnalium) [3], primarily mechanical, is an urgent task. These alloys are not heat-strengthened, and therefore the main approach to improving their strength properties is strain hardening. In recent years, numerous studies have demonstrated that severe plastic deformation (SPD) by high pressure torsion (HPT) significantly increases the strength characteristics of most aluminum alloys due to the formation of nanocrystalline and ultrafine-grained structures in them [4]. At the same time, the analysis of hardening mechanisms results in the understanding of the fundamental limitations for known alloys. At the same time, it opens up opportunities to achieve even higher strength characteristics of magnaliums by improving existing and creating new metal matrix composites (MMC) of the Al−Mg system with a higher magnesium content (over 13 mass.%), since an increase of the content of this dopant significantly increases the strength of the material [5]. So, each percentage of magnesium in magnaliums results in an increase of the value of the ultimate strength by 30 MPa [3]. Powder metallurgy methods commonly used for mechanical alloying and composite materials production are multi-stage and lead to unavoidable contamination of components and, ultimately, do not ensure high strength characteristics [6]. There are other methods of manufacturing aluminum-based MMC, for example, metal melt impregnation of a porous billet from the dispersed phase, casting composites in which the reinforcing frame is formed from eutectic and intermetallic particles [7], spray molding, injection molding or mixing [8], cumulative rolling [9], explosion welding [10], friction stir welding , etc. All these methods involve, as a rule, the use of relatively low pressures and elevated temperatures for a long time. On the contrary, HPT is based on extremely large plastic deformation under quasi-hydrostatic conditions and is characterized by the greatest shear deformations in the material without destruction for a short period of time, which makes it possible to obtain nanocrystalline and ultrafine-grained structures even in low-plastic materials at room temperature [11,12]. Significant hardening as a result of SPD is ensured by the combined action of several mechanisms such as grain boundary, dislocation, solid-solution and dispersion hardening [5].

Previous studies have shown that MMC obtained by the HPT method have improved mechanical and physical properties in comparison with MMC obtained by the conventional method, which makes them promising for further R&D activities [10–12]. Such MMC are often referred to as metal hybrids since the HPT method allows combining dissimilar metals at room temperature to form formation of heterogeneous structures in cross-section characterized not only by a gradient distribution of grain size from the larger grains in the center to ultrafine grains in the periphery, by a heterogeneous distribution of secondary phase particles, but also by a heterogeneous distribution of many structure-sensitive properties, such as microhardness [13]. This method was used for fabrication of metal matrix composites based on Al−Cu [13–16],

Al–Ti [13,17,18], Al–Mg [13,19–21] and other various systems including even such compositions as Al–Nb, which is difficult to obtain by fusion because of the significant difference of melting temperatures [22]. The main advantage of HPT processing is the possibility of obtaining composites without contamination and residual porosity in one process step at room temperature. The introduction of hardening particles into composites, for example, Al_2O_3, improves the complex mechanical properties of composites in comparison with aluminum, in particular, the wear resistance [23]. The paper [24] describes the fabrication of MMC using the SPD method with SiC particles for hardening of the aluminum matrix. The resulting material showed increased hardness and elastic modulus compared to pure aluminum. The introduction of TiB_2 nanoparticles into the aluminum matrix composite not only improves the thermal stability of the composite and prevents grain growth during heating, but also allows achieving high elongations in the superplasticity mode [25]. There is evidence that composites with inclusions of graphene and carbon nanotubes made by the HPT method demonstrate increased strength and ductility compared to aluminum [26,27]. In general, these studies demonstrate the potential of HPT as an effective method for obtaining MMC with improved mechanical properties, and the use of various reinforcing particles and processing parameters by SPD methods can result in further improvement of the MMC properties.

At the same time, the mechanical properties were evaluated by microhardness measurements in most studies, since the size of composite samples obtained by the HPT method is small. The results of mechanical tensile tests of proportional specimens cut out from MMC obtained by the HPT method with different degrees of deformation are presented in this paper along with microhardness data.

The aim of this paper is to study the evolution of the microstructure and mechanical properties of a metal-matrix composite of the Al–Mg system in case of deformation by HPT method using an increased pressure of 8 GPa and varying the speed from $n = 10$ to 100.

1. Materials and research techniques

The study materials were aluminum (AD0) with a grain size of 10–30 μm and magnesium (MA2-1) with a grain size of 10 μm. The initial aluminum and magnesium billets were cut out in the form of disks with a diameter of 12 mm and a thickness of 1 and 0.3 mm, respectively. Disk blanks were pre-ground to remove dirt and obtain a smooth surface: aluminum blanks were ground in running water, magnesium blanks were ground in ethyl alcohol. Intense plastic deformation by high-pressure torsion was applied for obtaining samples of Al–Mg composite. Bridgman anvils with recesses in their center of 0.25 mm and a diameter of 12 mm were used in the experiment. The initial metal billets were stacked in the form of a sandwich in the sequence Al–Mg–Al. Torsional deformation was performed at a press force equal to 1200 kN, which corresponded to a pressure of at least 8 GPa. The torsional pressure remained constant. The speed of revolutions of the anvils was set to 3 rotations per minute, the number of rotations n ranged from 10 to 100. The specimens were heated no higher than 100°C in the process of rotation up to 100 rotations, [28]. Disk samples of composites with a diameter of 12 mm and a thickness of about 0.6–0.7 mm were obtained as a result of deformation. Annealing was performed at 275°C for half an hour. The samples were placed in a preheated furnace, they were removed from the furnace after the annealing time and were cooled in air. The temperature and annealing time were selected based on the analysis of differential scanning calorimetry data in such a way as to ensure the primary recrystallization and prevent the release of intermetallic phases, since such phases cause embrittlement of the composite, which was previously revealed by us [21].

Microstructure, chemical and phase compositions, and microhardness measurements were performed on a cross-section of composite samples. Disk samples (after deformation) were cut along the diameter into two parts for this purpose. The microstructure and phase composition were studied using a Tescan Mira 3LHM scanning electron microscope with EDX detector and Rigaku Ultima IV X-ray diffractometer with Cu–K_α-radiation. The phase composition was evaluated by the Rietveld method using the MAUD software package. Microhardness was measured by the Vickers method using MHT-10 Paar Physica microhardness tester combined with Carl Zeiss optical microscope. The load was set to 25 g (0.25 N). The diamond pyramid indentation and exposure time was 10 s. Experimental data were processed with a confidence probability of 95%. At the same time, the relative measurement error did not exceed 10%.

Static tensile tests were performed to determine the mechanical properties of composite materials of the Al–Mg system obtained by HPT method. The geometry of the samples close to the requirements of GOST 1497-84 was specially developed for this purpose. Flat samples in the form of a double-sided blade with a working part length of 3 mm,a width of 1 mm, and a thickness of 0.55 mm were cut from disk samples with a diameter of 12 mm in the area between the center and the edge of the sample. Special grippers were made for holding such thin samples. This grippers allowed performing tests close to the requirements of GOST 1497-84 and determining the ultimate strength (σ_B, [MPa]) and elongation (δ, [%]) of the composite samples. The tests were performed on an electromechanical universal testing machine CMT-3 (Liangong Testing Technology Co) at room temperature with a strain rate of $5.5 \cdot 10^3\,s^{-1}$ until sample destruction. Four samples were tested for each structural state. The relative measurement error did not exceed 3%.

2. Findings and discussion

2.1. Evolution of composite microstructure in case of torsion under high pressure

Figure 1 shows cross-sectional images of composites obtained by torsion of three-layer Al−Mg−Al billets at 10, 50, and 100 anvil rotations. The light areas in the scanning electron microscope images correspond to the Al-based phase, while the dark areas correspond to the lighter Mg-based phase. It can be seen that the samples of all the obtained composites do not contain pores and cracks. The initial three-layer structure was significantly transformed as the layers were fragmented and mixed. In a sample with a lower number of rotations ($n = 10$), a two-phase structure is observed throughout the entire volume of the material, and the Mg-based phase has the form of layered fragments that are larger and located densely in the middle of the central zone of the disk sample and smaller, distributed more uniformly on the periphery. This reallocation is attributable to the fact that the shear strain depends on the distance from the center in case of HPT and is described by the formula [12]

$$\gamma = \frac{2\pi nR}{h}, \qquad (1)$$

where n — the number of rotations of the anvil, R and h — distance from the center and thickness of the sample, respectively. This means that the minimum shear strain occurs in the center of the disk, and the maximum is at its periphery. This dependence determines the gradient distribution of structural elements in the disk sample.

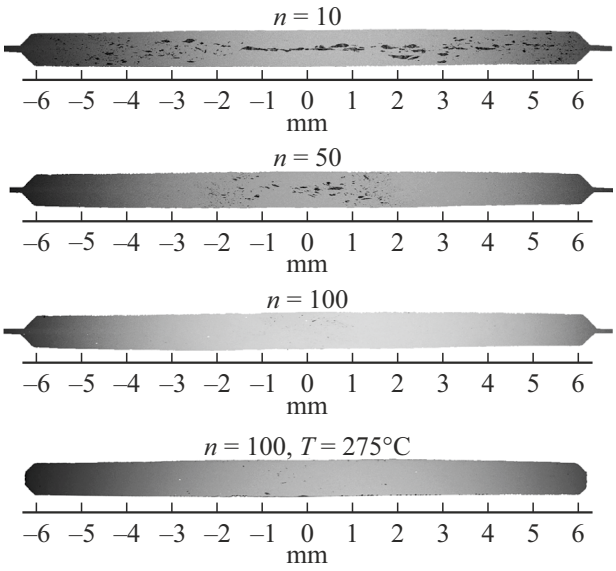

Figure 1. SEM images (BSE mode) of the cross-section of samples of composites of the Al−Mg system obtained by HPT method with different rotations: $n = 10$, 50 and 100, as well as after annealing at 275°C of the composite Al−Mg obtained with the number $n = 100$.

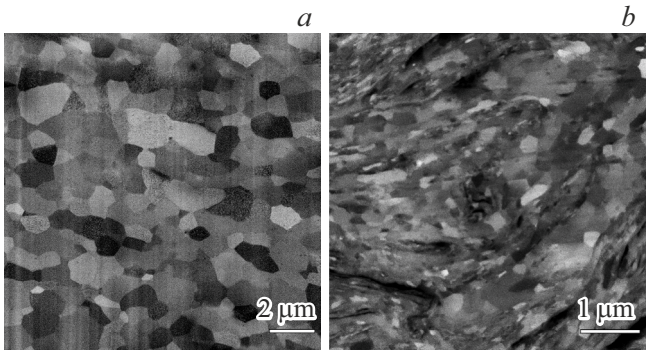

Figure 2. SEM images (BSE mode) of the cross-section of the peripheral zone of the composite of Al−Mg system obtained by HPT method at $n = 100$ rotations before annealing (a) and after annealing at 275°C (b).

The degree of deformation increases in the entire sample with an increase of the number of rotations ($n = 50$), according to the above formula, but it is greater in the peripheral zone, where fragments of Mg-based layers are almost completely dissolved ($n = 50$, Fig. 1). Almost the entire sample contains only the Al-based phase at the maximum number of rotations ($n = 100$) and a completely homogeneous structure is observed. Few fragmented magnesium salts are observed in aluminum only in the central part with a width of about 1 mm (Fig. 1). Studies using energy-dispersive X-ray spectroscopy indicate that the Mg distribution in the Al matrix turned out to be uniform and approached 5 weight%. After annealing at 275°C, the macrostructure in the composite with the maximum degree of deformation ($n = 100$) practically does not change.

Images taken with higher magnification on the composite periphery ($n = 100$) indicate the initial stage of dynamic recrystallization — recrystallized grains, the average size of which does not exceed 300 nm, occupy a small volume of the composite (Fig. 2, a), forming a mixed structure. Clearly distinguishable bends of structural elements are associated with the development of rotational modes of shear deformation at the boundaries of metal joints with different elastic and strength parameters. A more detailed description of rotational modes in multilayer structures that occur during shear under pressure is published in the papers on composites of the Al−Cu system [29,30]. The traces of rotational modes disappear after annealing at 275°C, the grain size increases to 2 μm, and the grain boundaries become straight, which is attributable to static recrystallization in the composite during annealing (Fig. 2, b).

Microstructural observations are confirmed by X-ray diffraction data. Figure 3, a shows fragments of diffractograms in the range of angles 36−39° recorded from the cross-section of composites obtained at $n = 10$, 50 and 100. Figure 3, b shows diffractograms of the same composites annealed at 275°C. It is well seen that there are practically no diffraction maxima corresponding to pure Mg in the

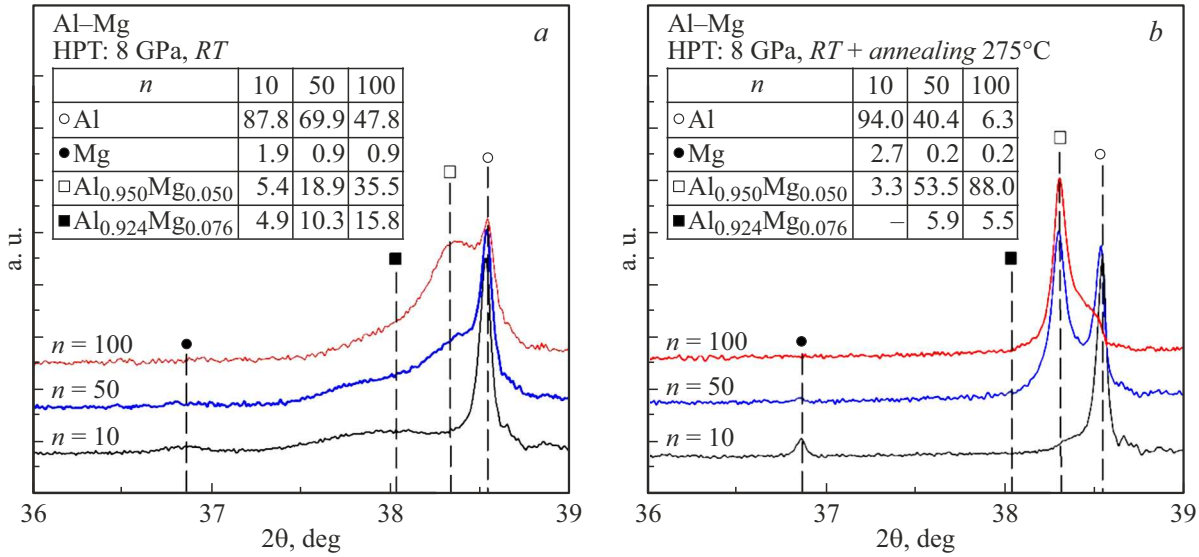

Figure 3. Fragments of the diffraction pattern and phase composition of composites of Al–Mg system obtained at $n = 10$, 50 and 100 rotations before annealing (this is a) and after annealing at 275°C (b).

composites (Fig. 3, a), and the maxima corresponding to Al have transformed into doublets, and there are blurred diffraction maxima to the left of the main lines along with clear reflections from pure aluminum Al(111) (Fig. 3, a). These reflections seem to be related to the formation of a solid Mg solution in Al. The shift of the diffraction maxima from the solid solution towards smaller angles indicates an increased value of the lattice parameter and corresponds to the known data [31,32]. An increase of the degree of deformation with an increase in the number of rotations leads to further fragmentation of Mg inclusions and their dissolution in Al. This process is accompanied by a decrease of the intensity of reflection from pure aluminum Al(111) and an increase of the intensity of diffraction maxima of the solid solution (Fig. 3, a).

Intermetallic phases are often formed during the interaction of two metals [33,34]. However, phase formation depends on the solubility region in the binary system, the atomic diffusion coefficients, thermodynamic parameters,and the time of the process. The growth of a particular phase depends on the diffusion coefficient of atoms inside its lattice and in neighboring phases from the diffusion point of view, when two phases are adjacent to each other. The rate of diffusion depends, among other things, on the grain size, vacancy density, and dislocations. A significant density of pointed and linear defects is generated under conditions of intense shear deformation, which significantly changes the diffusion kinetics of the components. In addition, each atom of one component is surrounded by the maximum number of atoms of the other component in systems with a negative mixing enthalpy. In our case, the joint deformation of Al and Mg under conditions of quasi-hydrostatic compression without external heating leads to the diffusion of Al into Mg and Mg into Al, which is followed by the formation of a solid solution of variable composition, covering, with increasing degree of deformation, larger volumes of material. This is associated with a decrease of the intensity of reflections from pure aluminum Al (111) and an increase of the intensity of the blurred peak of the Al–Mg(111) solid solution with an increase of the degree of deformation (Fig 3, a).

As a result of subsequent annealing, a clear diffraction maximum corresponding to an Al solid solution with 5% Mg ($Al_{0.95}Mg_{0.05}$) and a small maximum associated with Al with 8% Mg ($Al_{0.92}4Mg_{0.076}$) are formed on diffractograms of composites obtained by turning the anvil by 50 and 100 rotations, along with reflection from pure Al (Fig. 3, b). The content of pure Al turned out to be about 6% in the sample $n = 100$ after annealing and the proportion of solid solution exceeded 90%. The expected noticeable diffraction maxima from the intemetallic phases were not detected. It should be noted here that intermetallic phases β-Al_3Mg_2 and γ-$Al_{12}Mg_{17}$, located predominantly along the Al/Mg interfaces, were found in the composite obtained by using a lower number of rotations ($n < 50$), as in our previous paper [21], where lower pressure and speed were used($P = 5$ GPa, $n = 10$). Similar results were previously presented in the papers of M. Kawasaki [13,20] in Al–Mg composite obtained at a pressure of 6 GPa and 20 anvil rotations, where the formation of intermetallic phases (mainly $Al_{12}Mg_{17}$ and a small fraction of Al_3Mg_2), as well as the formation of a solid solution of Al with 7% Mg after annealing at 300°C.

Thus, when the number of rotations is increased to $n = 100$ and a pressure of more than 8 GPa is used, it is possible to form a nanocrystalline structure consisting mainly of pure aluminum and a solid solution. After

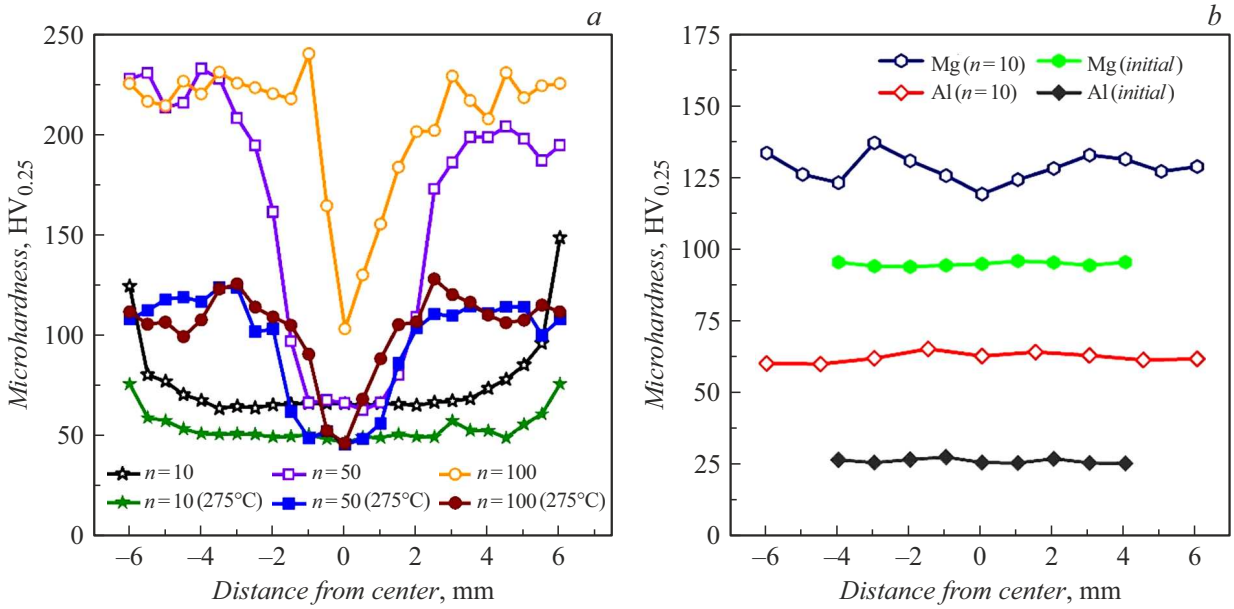

Figure 4. Microhardness distribution in Al−Mg composite obtained by HPT method with different number of rotations before annealing and after annealing at 275°C for 30 min (*a*), microhardness distribution in pure Al and Mg in the initial coarse-grained state and after HPT ($n = 10$) (*b*).

annealing, almost the entire composite is a solid solution of Mg in Al, and X-ray diffraction patterns do not detect the presence of inclusions of intermetallic phases.

2.2. Evolution of composite microhardness in case of torsion under pressure

The microhardness (HV) of composites obtained at different degrees of deformation was measured for evaluation of the composite hardening, as well as to visually reveal its macroscopic homogeneity. The microhardness distribution along the diameter measured in the middle part of the composite cross-section before and after annealing is shown on Fig. 4, *a*. The microhardness values for pure Al and Mg in the initial coarse-grained state, as well as those subjected to HPT with $n = 10$ are given for comparison in Fig. 4, *b*.

It is clearly seen that the composite HV practically does not differ from pure aluminum HV after a slight deformation ($n = 10$). The values of the composite HV increase almost by 3 times with an increase of the degree of deformation ($n = 50$, 100), but the microhardness values are much lower in the central zone of composites, and the diameter of this zone decreases with an increase of the degree of deformation, but it is not possible to achieve a completely uniform microhardness distribution in the composite even at $n = 100$ because the center zone is subject to weaker deformation according to formula (1). It should be noted here that the microhardness distribution in pure Al and Mg is uniform, and the HV values are marginal for $n = 10$ [12]. This is consistent with the known data on the relationship of microhardness after HPT with the homologous temperature T/T_{melt} (where T — deformation temperature, T_{melt} — melting point) for a large number of pure metals [35]. Metals with $T/T_{melt} > 0.4$ undergo softening during HPT process, while metals with $T/T_{melt} < 0.25$ undergo significant irreversible hardening [36]. $T/T_{melt} = 0.32$ for Al and Mg, and the process is reversed during HPT in these metals, which reduces the level of internal stresses and does not allow the material to strengthen above certain values, but provides a relatively uniform distribution of HV [37]. Obviously, the high energy of stacking faults in pure Al facilitates the transverse sliding of dislocations, which ensures a high rate of recovery and a uniform distribution of HV. In contrast to pure Al in aluminum alloys, the energy value of stacking faults is lower and the recovery processes occur at lower speeds. Therefore, the recovery and relaxation of internal stresses does not occur at the required rate, and a significant increase of HV is observed in composites obtained at $n = 50$ and 100, where a solid solution of Al−Mg was formed as a result of significant mutual diffusion of Al and Mg.

It should be noted here that the obtained HV values for composites obtained at a high degree of deformation ($n = 50$ and 100) significantly exceed the HV values for pure Al and Mg. This does not agree with the empirical rule of additivity for laminar structures [38], according to which the HV of a composite is determined by the volume fraction and HV of individual components and cannot exceed the HV of the strongest component. All this points to different hardening mechanisms in composites and pure metals.

In pure metals, the main contribution to hardening, along with point and linear lattice defects, is made by grain boundaries [5] — Hall−Petch strengthening mech-

anism [39,40], according to which the yield strength is inversely proportional to the grain size. This contribution for pure Al and Mg is limited due to the relatively high homologous temperature. At the steady-state stage of deformation in HPT, the grain size and, consequently, the hardness remain constant due to the balance between the accumulation of dislocations and grain grinding, on the one hand, and the annihilation of dislocations and the destruction of grain boundaries, on the other hand [37]. Such an equilibrium is achieved even with a small number of rotations, and after torsion by 3–4 rotations, the HV diameter distribution in pure Al becomes uniform [36].

In nanostructured aluminum alloys, as in pure Al, the main mechanism of hardening is attributable to the grain size. Additionally, there are mechanisms of deformation, solid-solution hardening and hardening due to dispersed inclusions. Therefore, higher HV values are achieved in composites obtained at high degrees of shear deformation ($n = 50$ and 100), where mutual diffusion of components occurred and a solid solution was formed, and it first occurs at the periphery of the composite, where the degree of deformation is maximum, and then the zone of high the hardness distribution extends to the center of the sample with an increase of the degree of deformation.

Thus, the use of high pressure (~ 8 GPa) and a large number of rotations (up to $n = 100$) in the HPT process made it possible to obtain composites of the Al–Mg system with a homogeneous structure in almost the entire volume of the disk sample, with the exception of the central zone with a diameter of not more than 2 mm. This result was not achieved in earlier studies in Ref. [41–43] at pressures 5–6 GPa and at a lower number of rotations, and the composites of Al–Mg system had an inhomogeneous structure with a gradient distribution of both grain size and phase composition.

2.3. Mechanical properties of composites of Al–Mg system

The table shows the results of mechanical tensile tests at room temperature of samples of composites of Al–Mg system obtained at $n = 10$, 50 and 100 before and after annealing. For comparison, the table also shows the results obtained for samples of pure Al and Mg in the initial coarse-grained state and after HPT with the number of rotations $n = 10$. The maximum tensile strength (σ_B) is demonstrated by Al–Mg composite obtained with the number of rotations $n = 100$, which is slightly less than the strength of the composite with the number of rotations $n = 50$. The value UTS of about 600 MPa obtained after HPT corresponds to the strength of high-strength aluminum alloys in the nanostructured state [5] and significantly exceeds the strength of pure Al and Mg (see table), as well as the strength of composites Al–Mg obtained earlier using a lower pressure and degree of deformation [21].

It is known that an increase of strength by deformation methods is usually accompanied by a drop of tensile elongation. This statement is valid for the Al–Mg composites obtained at $n = 10$ and 50. It can be seen (see table) that an increase of the number of rotations from $n = 10$ to 50 ensures an increase of the strength of the composite, but results in a decrease of elongation from 3.3% to almost zero value (0.1%). Not only a further increase of the strength of the composite is observed in the case of Al–Mg composite obtained at $n = 100$, but also the occurrence of some elongation (0.5%) compared to Al–Mg composite obtained at $n = 50$.

Mechanical tensile properties (tensile strength, UTS, [MPa] and elongation, δ, [%]) at room temperature of composites of Al–Mg system obtained by HPT method with different number of rotations (n) before annealing and after annealing at 275°C for 30 min, and properties of pure Al and Mg in the initial coarse-grained state and after HPT

Material	Condition	Quantity Revs (n) during HPT	UTS, MPa	δ, %
Al–Mg	HPT	10	189	3.3
		50	400	0.1
		100	604	0.5
Al–Mg	HPT+annealing	10	121	1.8
		50	141	11.6
		100	360	12.7
Al	Initial	–	66	57.0
Al	HPT	10	230	9.3
Mg	Initial	–	183	10.1
Mg	HPT	10	237	0.2

It is believed that nanostructured metallic materials have high flow stresses, but a low hardening rate due to the inability of nanocrystalline or ultrafine-grained grains to accumulate mobile dislocations, and the microstructure has a higher plasticity, providing more places for the accumulation of dislocations [44]. An important role in the dynamics of the dislocation distribution during deformation can also be played by various types of point defects, which are present in large quantities in metal lattices during intense deformation effects [45–47].

The ductility of the material is important primarily for application tasks as it is important both for shaping operations and for preventing fatigue failures during operation. Therefore, annealing was carried out at 275°C, after which the grain size in Al–Mg composite with $n = 100$ increased from 0. 3 to 1 μm (Fig. 2, *b*), and both Al–Mg composites

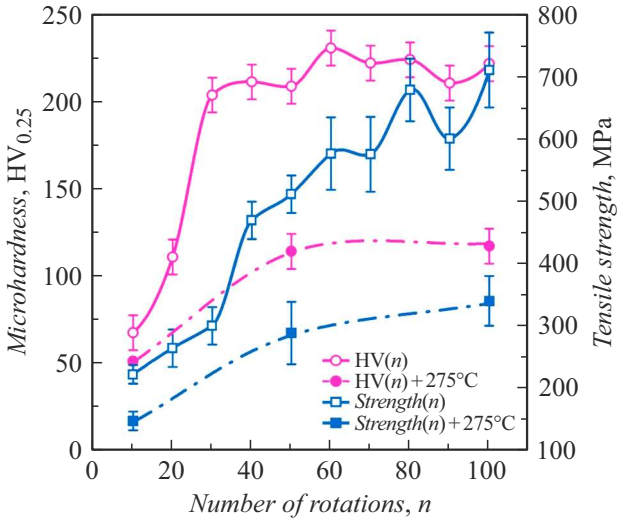

Figure 5. Effect of the number of rotations n in case of HPT on the microhardness and tensile strength of Al−Mg composites.

($n = 50$ and 100) exhibited an elongation of about 12%. It should be noted that Al−Mg composite obtained at $n = 100$, as well as in the case before annealing, has a higher elongation value compared to Al−Mg composite obtained at $n = 50$, 12.7% and 11.6%, respectively. However, the value of the ultimate strength of the annealed Al−Mg composite with $n = 100$ exceeds the value of the ultimate strength of the annealed Al−Mg composite with $n = 50$ by 5.6%.

Measurements of microhardness and tensile strength on a series of composite samples obtained at the number of rotations from $n = 10$ to 100 are shown in Figure 5. The microhardness values in the graph of the HV dependence on the anvil speed are obtained from measurements at a distance of 4 mm from the center of the disk samples, which corresponds to the working area of proportional tensile samples used for measuring UTS. The graphs in Figure 5 show a good correlation between microhardness and tensile strength. The increase of the number of rotations to $n = 40$ results in a significant increase of both HV and UTS. Further increase of the speed to $n = 80$ provides only a small increase of strength characteristics. No changes are observed at $n = 90$ and 100, which indicates the achievement of critical stresses and the steady-state stage of deformation, when the grain size and, consequently, strength characteristics practically do not change.

Conclusion

The example of light metal matrix composites of Al−Mg system obtained by intense plastic torsional deformation on Bridgman anvils was used to demonstrate that it is possible to obtain a high-strength state with a tensile strength of about 700 MPa by applying a high pressure of 8 GPa and a speed of 50 to 100 rotations which is attributable to the formation of a mixed partially recrystallized structure consisting mainly of pure aluminum and a solid solution of Mg in Al during intense deformation. A heterogeneous structure is formed in case of deformation with a number of rotations of 10. This structure consists of individual Mg interlayers in the Al matrix, the ultimate strength of such a composite is about 200 MPa. The increase of the microhardness and strength of composite samples after deformation is associated with the action of several hardening mechanisms-grain boundary, solid-solution, and dispersed hardening due to the occurrence of dispersed intermetallic phases, and the first two factors play a major role in the increase of the microhardness and strength of Al−Mg composites obtained with a high degree of deformation under torsion with 50 to 100 rotations.

Additional low-temperature heat treatment is necessary for obtaining a structural state with some plasticity. A homogeneous fine-grained structure of the solid solution is formed without embrittling intermetallic inclusions as a result of annealing at 275°C of samples deformed with a number of rotations from 50 to 100.

Thus, taking into account the previous experiments, it is possible to conclude that the varying of the deformation modes by selecting the pressure and speed and subsequent heat treatment allows obtaining a wide range of structural states with different levels of mechanical properties of the composite based on Al and Mg. A significant result is the found range of degrees of deformation corresponding to torsion at 50−100 rotations and ensuring the formation of a homogeneous structure at a given increased pressure of 8 GPa with a high level of mechanical properties corresponding to high-strength aluminum alloys, practically over the entire volume (with the exception of the stagnant zone).

Funding

Studies of the structure, physical and mechanical properties were carried out within the scope of the state assignment of the Institute of Metal Superplasticity Problems of the Russian Academy of Sciences. Composite samples were obtained during a project of the Russian Science Foundation (project No 18-12-00440). K. E. A. is grateful for the support of the Ministry of Science and Higher Education of the Russian Federation in the framework of the state assignment of the Ufa University of Science and Technology (№ 075-03-2023-119).

Conflict of interest

The authors declare that they have no conflict of interest.

References

[1] A.A. Luo, A.K. Sachdev, D. Apelian. J. Mater. Proces. Technol., **306**, 117606 (2022).
DOI: 10.1016/j.jmatprotec.2022.117606

[2] K. Lu. Science, **328** (5976), 319 (2010). DOI: 10.1126/science.118586
[3] K.V. Frolov, I.N. Friedlander, O.G. Senatorova, O.E. Osintsev. *Mashinostroenie. Entsiklopediya. V 40 t. Cvetnye metally i splavy. Kompozitsionnye metallicheskie materialy* (Mashinostroenie, M., 2001), t. 2–3 (in Russian).
[4] A.A. Nazarov, R.R. Mulyukov. *Nanostructred Materials.* In: *Handbook of NanoScience. Engineering and Technology* (CRC Press, Boca Raton, 2002), p. 22-1-22-41, DOI: 10.1201/9781420040623
[5] I. Sabirov, M.Y. Murashkin, R.Z. Valiev. Mater. Sci. Engineer.: A, **560**, 1 (2013). DOI: 10.1016/j.msea.2012.09.020
[6] S. Scudino, M. Sakaliyska, K.B. Surreddi, J. Eckert. J. Alloys and Compounds, **483** (1–2), 2 (2009). DOI: 10.1016/j.jallcom.2008.07.161
[7] T.K. Akopyan, N.A. Belov, E.A. Naumova, N.V. Letyagin. Mater. Lett., **245**, 110 (2019). DOI: 10.1016/j.matlet.2019.02.112
[8] B. Bihari, A.K. Singh. IJERA, **7**, 42 (2017). DOI: 10.9790/9622-0701034248
[9] V.Y. Mehr, M.R. Toroghinejad, A. Rezaeian. Mater. Sci. Engineer., **601**, 40 (2014). DOI: 10.1016/j.msea.2014.02.023
[10] D.M. Fronczek, R. Chulist, L. Litynska-Dobrzynska, G. Lopez, A. Wierzbicka-Miernik, N. Schell, Z. Szulc, J. Wojewoda-Budka. Mater. Design, **130**, 120 (2017). DOI: 10.1016/j.matdes.2017.05.051
[11] R.Z. Valiev, A.V. Korznikov, R.R. Mulyukov. Mater. Sci. Engineer.: A, **168** (2), 141 (1993)
[12] A.P. Zhilyaev, T.G. Langdon. Progr. Mater. Sci., **53** (6), 893 (2008). DOI: 10.1016/j.pmatsci.2008.03.002
[13] D. Hernández-Escobar, M. Kawasaki, C.J. Boehlert. Intern. Mater. Rev., **67** (3), 1 (2022). DOI: 10.1080/09506608.2021.1922807
[14] O. Keiichiro, K. Edalati, H.S. Kim, K. Hono, Z. Horita. Acta Mater., **61** (9), 3482 (2013). DOI: 10.1016/j.actamat.2013.02.042
[15] O. Bouaziz, H.S. Kim, Y. Estrin. Adv. Engineer. Mater., **15** (5), 336 (2013). DOI: 10.1002/adem.201200261
[16] R.R. Mulyukov, G.F. Korznikova, K.S. Nazarov, R.Kh. Khisamov, S.N. Sergeev, R.U. Shayachmetov, G.R. Khalikova, E.A. Korznikova. Acta Mechanica, **232**, 1815 (2021). DOI: 10.1007/s00707-020-02858-6
[17] Y. Sun, M. Aindow, R.J. Hebert, T.G. Langdon, E.J. Lavernia. J. Mater. Sci., **52**, 12170 (2017). DOI: 10.1007/s10853-017-1331-z
[18] A. Bartkowska, P. Bazarnik, Yi Huang, M. Lewandowska, T. Langdon. Mater. Sci. Engineer.: A, **799**, 140114 (2021). DOI: 10.1016/j.msea.2020.140114
[19] M. Kawasaki, J.-K. Han, D.H. Lee, J. Jang, T.G. Langdon. J. Mater. Res., **33**, 2700 (2018). DOI: 10.1557/jmr.2018.205
[20] J.-K. Han, H.-J. Lee, J.-I. Jang, M. Kawasaki, T.G. Langdon. Mater. Sci. Engineer.: A, **684**, 318 (2017). DOI: 10.1016/j.msea.2016.12.067
[21] G.F. Korznikova, E.A. Korznikova, G.R. Khalikova, K.S. Nazarov, R.K. Khisamov, S.N. Sergeev, R.U. Shayakhmetov, R.R. Mulyukov. Lett. Mater., **11** (4s), 533 (2021). DOI: 10.22226/2410-3535-2021-4-533-543
[22] G. Korznikova, E. Korznikova, K. Nazarov, R. Shayakhmetov, R. Khisamov, G. Khalikova, S. Sergeev, R. Mulyukov. Adv. Engineer. Mater., **23** (1), 2000757 (2021). DOI: 10.1002/adem.202000757
[23] K. Edalati, M. Ashida, Z. Horita, T. Matsui, H. Kato. Wear, **310** (1–2), 83 (2014). DOI: 10.1016/j.wear.2013.12.022
[24] Y. Xie, Y. Huang, F. Wang, X. Meng, J. Li, Z. Dong, J. Cao. J. Alloys Compounds, **823**, 153741 (2020). DOI: 10.1016/j.jallcom.2020.153741
[25] Q. Zhang, X. Ju, J. Liu, L. Wang, Y. Li, H. Wang, Z. Chen. Mater. Characterization, **182**, 111531 (2021). DOI: 10.1016/j.matchar.2021.111531.
[26] P. Lava Kumar, A. Lombardi, G. Byczynski, S.V.S. Narayana Murty, B.S. Murty, L. Bichler. Progr. Mater. Sci., **128**, 100948 (2022). DOI: 10.1016/j.pmatsci.2022.100948.
[27] V. Khanna, V. Kumar, S.A. Bansal. Mater. Today: Proceed., **38** (1), 289 (2021). DOI: 10.1016/j.matpr.2020.07.221.
[28] K.S. Nazarov, G.F. Korznikova, R.Kh. Khisamov, R.R. Timiryaev, E.A. Korznikova, G.R. Khalikova, R.U. Shayakhmetov, S.N. Sergeev, R.R. Kabirov, R.R. Mulyukov. Lett. Mater., **12** (4), 360 (2022). DOI: 10.22226/2410-3535-2022-4-360-366
[29] R. Kulagin, Y. Beygelzimer, Yu. Ivanisenko, A. Mazilkin, B. Straumal, H. Hahn. Mater. Lett., **222**, 172 (2018). DOI: 10.1016/j.matlet.2018.03.200
[30] G. Korznikova, R. Kabirov, K. Nazarov, R. Khisamov, R. Shayakhmetov, E. Korznikova, G. Khalikova, R. Mulyukov. JOM, **72**, 2898 (2020). DOI: 10.1007/s11837-020-04152-1
[31] L.F. Mondolfo. *Struktura i svojstva alyuminievyh splavov* (Metallurgiya, M., 1979) (in Russian).
[32] G.F. Lovshenko, E.I. Marukovich. Lit'e i metallurgiya, **2** (34) (in Russian). 156 (2005).
[33] S. Sanamar, H.-G. Brokmeier, N. Schell. J. Alloys Compounds, **911**, 165114 (2022). DOI: 10.1016/j.jallcom.2022.165114
[34] J. Tang, L. Chen, G. Zhao, C. Zhang, L. Sun. J. Magnesium Alloys, **8** (3), 654 (2020). DOI: 10.1016/j.jma.2020.02.016
[35] D. Dietrich, D. Nickel, M. Krause, T. Lampke, M.P. Coleman, V. Randle. J. Mater. Sci., **46**, 357 (2011). DOI: 10.1007/s10853-010-4841-5
[36] M. Kawasaki. J. Mater. Sci., **49**, 18 (2014). DOI: 10.1007/s10853-013-7687-9
[37] K. Edalati, Z. Acta Mater., **59** (17), 6831 (2011). DOI: 10.1016/j.actamat.2011.07.046
[38] X.L. Ma, C.X. Huang, W.Z. Xu, H. Zhou, X.L. Wu, Y.T. Zhu. Scripta Mater., **103**, 57 (2015). DOI: 10.1016/j.scriptamat.2015.03.006
[39] E.O. Hall. Proceed. Phys. Society. Section B, **64** (9), 747 (1951). DOI: 10.1088/0370-1301/64/9/303
[40] N.J. Petch. J. Iron and Steel Institute, **174**, 25 (1953).
[41] W. Jiang, H. Zhou, Y. Cao, J. Nie, Y. Li, Y. Zhao, M. Kawasaki, T.G. Langdon, Y. Zhu. Adv. Engineer. Mater., **22** (1), 1900477 (2020). DOI: 10.1002/adem.201900477
[42] R.Kh. Khisamov, R.U. Shayakhmetov, Y.M. Yumaguzin, A.A. Kistanov, G.F. Korznikova, E.A. Korznikova, K.S. Nazarov, G.R. Khalikova, R.R. Timiryaev, R.R. Mulyukov. Appl. Sci., **13** (8), 5007 (2023). DOI: 10.3390/app13085007
[43] G. Khalikova, G. Korznikova, K. Nazarov, R. Khisamov, S. Sergeev, R. Shayakhmetov, E. Korznikova, R. Mulyukov. AIP Conf. Proceed., **2533** (1), 020001 (2022). DOI: 10.1063/5.0098871
[44] Y.T. Zhu, X.L. Wu. Mater. Today Nano, **2**, 15 (2018). DOI: 10.1016/j.mtnano.2018.09.004

[45] E.A. Korznikova, S.Yu. Mironov, A.V. Korznikov, A.P. Zhilyaev, T.G. Langdon. Mater. Sci. Engineer.: A, **556**, 437 (2012). DOI: 10.1016/j.msea.2012.07.010
[46] E.A. Korznikova, I.A. Shepelev, A.P. Chetverikov, S.V. Dmitriev, S.Yu. Fomin, K. Zhou. J. Experimental Theor. Phys., **127**, 1009 (2018). DOI: 10.1134/S1063776118120063
[47] I. D. Kolesnikov, I. A. Shepelev. Mater. Technol. Design, **4** (1(7)), 5 (2022).

Translated by A.Akhtyamov